

# Dentin caries activity status related to hardness and elasticity

Zheng L, Hilton JF, Habelitz S, Marshall SJ, Marshall GW. Dentin caries activity status related to hardness and elasticity. *Eur J Oral Sci* 2003; 111: 243–252. © Eur J Oral Sci, 2003

This research tested the hypothesis that active and arrested carious dentin lesions have distinct structural characteristics and differ in atomic force microscopy-based nano-mechanical properties of the identifiable zones found in hydrated coronal carious lesions. Eight carious molars were used in this study. After longitudinally bisecting all the samples through the centers of carious lesions, they were divided into two sub-groups: moderately active caries and arrested caries. The samples were highly polished and stained by caries detector, which allowed identification of four zones: pink, light pink, transparent and apparently normal. The mechanical properties were studied wet using atomic force microscopy. The results show that both groups contained the same zones, regardless of activity status, and different zones have different mechanical properties. Generally, the more demineralized outer zones (pink, light pink) were larger and the mechanical properties of the zones were lower for moderately active caries. For arrested caries, the transparent zone occupied a larger portion of the lesion and the reduced elastic modulus was not significantly different from the underlying normal zone, although its hardness was lower than the apparently normal zone.

Lei Zheng<sup>1</sup>, Joan F. Hilton<sup>2</sup>,  
Stefan Habelitz<sup>1</sup>, Sally J. Marshall<sup>1</sup>,  
Grayson W. Marshall<sup>1</sup>

<sup>1</sup>Division of Biomaterials and Bioengineering, Department of Preventive and Restorative Dental Sciences; <sup>2</sup>Department of Epidemiology and Biostatistics, University of California, San Francisco, CA, USA

Dr Grayson W. Marshall, University of California, San Francisco, Department of Preventive and Restorative Dental Sciences, 707 Parnassus Avenue, San Francisco, CA 94143-0758, USA

Telefax: +1-415-4760858  
E-mail: graymar@itsa.ucsf.edu

Key words: carious activity; carious zones; caries detector; nanoindentation; atomic force microscopy

Accepted for publication February 2003

Carious coronal dentin was described by FUSAYAMA (1) as consisting of two distinct layers (an outer infected layer, and an inner affected layer). The inner layer contains collagen fibrils that retain their banded structure and intermolecular crosslinks, is uninfected, and is considered to be physiologically remineralizable (2). Conservative dental treatment seeks to remove the outer layer in which the collagen structure has been irreversibly lost, while retaining all potentially remineralizable dentin (3); however, recent work suggests that remineralization of the infected dentin also may be possible (4, 5). Clinical identification of the affected layer is problematic, since it is difficult to rely only on color change and tactile sensation to determine the point of minimal acceptable tissue removal. This difficulty is further exacerbated by limited and controversial guidance concerning the mechanical properties of several zones, which include a transparent zone in which dentin tubule lumens are partly to completely filled with mineral, and subtransparent and apparently normal zones under the transparent zone. The transparent zone is widely considered to be harder than normal dentin and is therefore often the target layer to discontinue excavation. However, it has been reported that the transparent zone can be softer than normal dentin (6) or have similar properties to normal dentin (7). Similar results for deciduous carious dentin have recently been reported by HOSOYA *et al.* (8). These findings suggest that excessive removal of tooth tissue is common and seems to be inevitable. In an effort to solve this problem, FUSAYAMA & TERACHIMA (9)

developed a caries detector solution composed of a propylene glycol solution (1,2-propanediol) with acid red 52 that reportedly could differentiate the two layers by staining the outer layer pink. SANO (10) found that the staining was based on penetration into highly porous demineralized tissue, regardless of bacterial infection. Although use of this stain clinically has been criticized as being insufficiently discriminating (11), it is clear, based on degree of staining, that the carious dentin lesion can be classified into pink, light pink, transparent, and apparently normal zones. These four zones have distinct mechanical properties, which may guide clinical decisions to excavate or remineralize dentin (7).

Dentin hardness has been a traditional measure of mineralization of the tissue, while elastic modulus is a fundamental materials property; both are important to understand the mechanical properties of calcified tissue and alterations caused by caries. Most research on carious dentin has been performed under dry conditions using microhardness. These studies have significant shortcomings because microhardness values represent composite averages for the various components of the dentin, the fundamental elastic modulus is not usually determined, and demineralized dentin is known to undergo drastic shrinkage when dried (12), which alters its properties (13). Nano-indentation has recently been used for the examination of tooth structure (14), and when used with modified atomic force microscopy (AFM) allows high-resolution imaging of hydrated samples and site-specific measurements of both hardness

and reduced elastic modulus (13,15–18). MARSHALL *et al.* (7) recently used this method to determine the hardness and reduced elastic modulus of carious zones, but did not classify the activity status of the lesions. Clinical guidelines suggest that more active lesions are light in color and soft, while less active or arrested lesions are dark and relatively harder. However, this characteristic sometimes cannot be correlated with the hardness of a lesion, thus, the extent to which active and inactive caries specimens differ in hardness and elastic modulus is not known (5).

In order to more fully understand the various characteristic zones and their relationship to the caries activity status, we undertook this study of hydrated coronal carious lesions using AFM. The purpose of this research was to test the hypothesis that active and arrested carious lesions have distinct structural characteristics that vary with respect to relative zone sizes and, may differ in their AFM-based nano-mechanical properties.

## Material and methods

### Selection of teeth for study

Subjects that contributed molars for this research provided informed consent for the protocol, which had been approved by the UCSF Institutional Committee on Human Research. The extracted teeth, which contained no prior restorations, were sterilized by gamma radiation (19) and stored in Hank's balanced salt solution at 4°C (20). This precluded evaluating the penetration of bacteria in the lesions. After longitudinally bisecting a sample through the center of its lesion using a water-cooled saw (Isomet Low Speed saw; Buehler, Lake Bluff, IL, USA) with a 0.15-mm thick diamond blade, a molar found to have an obvious carious lesion that appeared, by eye, to extend into the dentin by 50–75% of the dentin thickness was eligible for study. A 2-mm thick longitudinal section through the center of the lesion was polished, sequentially, using waterproof silicon carbide papers under running water with grit sizes of 600, 800, and 1200 and diamond pastes of 6, 3, 1 and 0.25  $\mu\text{m}$ . The prepared surface was stained by Caries Detector (Kuraray, Osaka, Japan). Additional specimens were prepared as described above until four exhibiting moderately active caries (slightly discolored; soft consistency; deeply stained by Caries Detector) and four exhibiting arrested caries (heavily discolored; hard consistency; lightly stained by Caries Detector) were identified. A digital image of the prepared surface of each of the eight specimens in the study sample was recorded (Scan Jet 4c Scanner; Hewlett Packard, Palo Alto, CA, USA).

### Classification of dentin zones

Four zones were identified in the lesions based on the appearance under the atomic force microscope, and the degree of staining of the dentin with Caries Detector: pink (nearest the dentino-enamel junction, DEJ), light pink, transparent, and an apparently normal zone (nearest the pulp). These zones were relatively distinct to the naked eye in arrested caries specimens but were not as obvious in the moderately active caries (Figs 1 and 2). Each zone had distinct microstructural features (6,7). In the AFM in the apparently normal zone, the intertubular dentin (ID) was smooth, peritubular dentin (PD) was present, and the

tubules were patent (not filled with intratubular mineral, ITM). In the transparent zone, the tubules were mostly filled with ITM and the ID was coarser. In the light pink zone, ITM partly filled the tubules, the PD was narrow or absent, and the ID was coarser. Finally, in the pink zone, PD and ITM were absent (see Figs 3 and 4 for typical microstructures). However, there are larger and more active lesions that were not included in the present study. Deeper lesions that reached to or very near the pulp, did not contain all four of the zones, and were not evaluated in this study. It should be noted that over half the lesions originally selected for possible inclusion in the active caries group were excluded from the study on the basis of probable pulpal involvement. Thus, we have used the term moderately active caries to describe the smaller lesions evaluated in this work.

### Measurement of reduced elastic modulus and hardness of dentin

A Nanoscope III AFM (Digital Instruments, Santa Barbara, CA, USA) modified with Triboscope head (Hysitron, Minneapolis, MN, USA) (7,13) was used to study the mechanical properties of zones in each lesion under wet conditions. A Berkovich diamond tip was used for the indentations, which were performed in a liquid cell filled with deionized water. All measurements used a trapezoidal force profile with peak loads between 300  $\mu\text{N}$  and 800  $\mu\text{N}$  and 3 s indentation times. Each indentation yielded a load-deformation curve, from which the reduced elastic modulus,  $E$ , was calculated from the slope of the unloading curve and the hardness,  $H$ , was determined according to the following equations (21):

$$E = \frac{\sqrt{\pi}}{2\sqrt{a}} S$$

$$H = \frac{F_{\max}}{a}$$

where  $S$  is the stiffness or slope of the unloading curve based on the method of OLIVER & PHARR (22),  $a$  is the contact area of the indentation, and  $F_{\max}$  is the maximum force. Measurements of reduced elastic modulus and hardness of the polished specimen were collected in two sets: linear data set and planar data set.

*Linear data set* – Indentations in the intertubular dentin were made at approximately equal intervals along the line traversing the center of the lesion (100  $\mu\text{m}$  to 160  $\mu\text{m}$ , depending on the tooth), from near the pulp chamber to the outermost point of the carious lesion at which the indentation was sharp and well-defined, and the load-displacement curve of the indentation showed no anomalous behavior. The outer portion of the pink layer of the dentin for moderately active caries was too soft for such measurements. When the DEJ was present, the dentinal depth was measured by using a digital caliper. When the DEJ was absent, which was common in the moderately active carious specimens, the lesion-free portion of the tooth was used as a guide to its location and the dentinal depth was estimated from the stained digital image using an image analysis program (NIH Image, <http://rsb.info.nih.gov/ij/>). The location of each indentation along the DEJ-to-pulp line was classified under the AFM, into one of the four zones described above based on the microstructural characteristics of the location of each indentation.

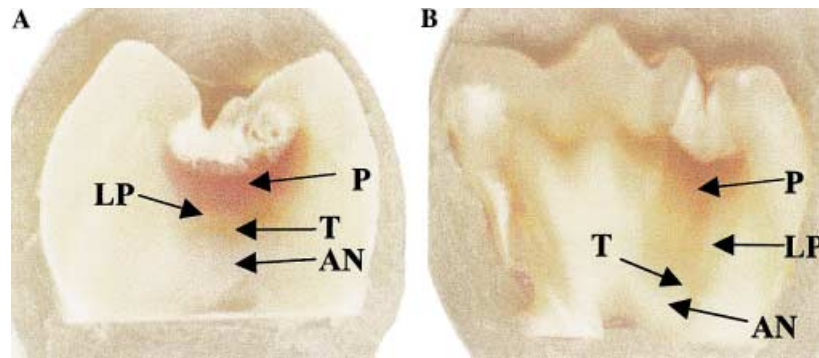


Fig. 1. Low-magnification digital images of arrested carious lesions stained by Caries Detector. (A) The lesion was divided into four zones based on the staining: pink, light pink, transparent and apparently normal. (B) This lesion appeared to be dark brown, and was barely stained by Caries Detector. P, pink zone; LP, light pink zone; T, transparent zone; AN, apparently normal zone.

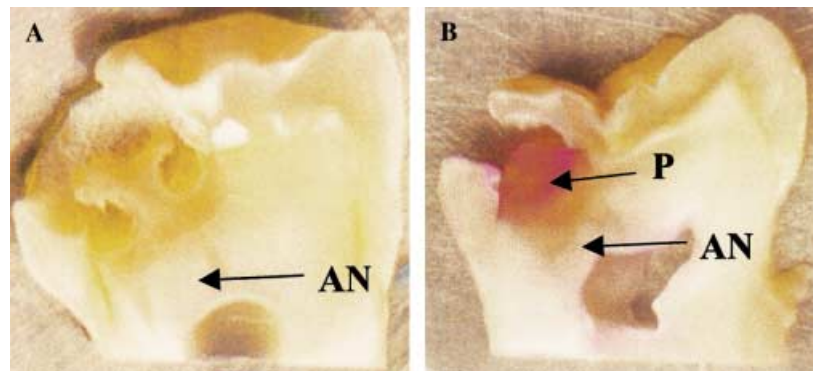


Fig. 2. Low-magnification digital images of moderately active carious lesions. (A) Unstained lesion for moderately active caries, which was slightly discolored and some tissue was lost owing to caries. (B) The image shows the stained moderately active carious lesion, which stained more intensely than arrested carious cases. P, pink zone; AN, apparently normal zone.

**Planar data set** – In the same eight teeth, indentations were made at 10 or more randomly selected locations within each zone, as identified under the AFM. At each location, more than two indentations were made within the PD that surrounded the tubules, ID and ITM individually (if PD and ITM were present) in order to determine the average hardness and reduced elastic modulus. The AFM images were collected before and after the indentations to ensure that they were uniform and well defined at each site.

### Statistical methods

Within each data set, outliers were identified by examining scatter plots of reduced elastic modulus by hardness and correcting or excluding erroneous values. The correlation between reduced elastic modulus and hardness was estimated, overall, in each data set.

**Linear data set** – Where tissue was missing or was too soft to measure, reduced elastic modulus and hardness were imputed based on linear extrapolations between the most superficial measured values and the implied DEJ location, at which point the values were assumed to be zero. In order to compare properties across teeth, the locations of the indentations along the DEJ-to-pulp line were expressed as fractions of the total dentinal depth for each tooth. A locally

weighted regression procedure was used to estimate the mean shapes (95% confidence intervals) of the hardness and reduced elastic modulus curves as quadratic polynomial functions of dentinal depth, by tooth and by caries status (proc loess; SAS, Cary, NC, USA). This non-parametric procedure is suitable for estimating a regression surface when its shape is unknown or irregular. When the effects of various smoothing parameters (0.3, 0.6, and 0.9) on the fits of the caries-specific models were evaluated, the best fits were obtained using a value of 0.6, according to residual analyses. For each tooth, hardness and reduced elastic modulus were plotted as functions of dentinal depth, and the depths at which zonal transitions occurred were marked by vertical lines (proc gplot; SAS). Similar plots were created to show the average relationships, for arrested caries and for moderately active caries, of hardness, reduced elastic modulus, and zone length with dentinal depth. Demarcations of zones were not included in the average curves because each sample had unique boundaries for each zone.

Mixed effects models were used to test for variation in the properties (hardness and reduced elastic modulus) by caries status within each zone (as a four-level nominal variable), allowing for interaction between caries and zone (SAS proc mixed; two-sided Wald tests). Specimens were distinguished in the models and included as random effects to account for correlation among indentations.

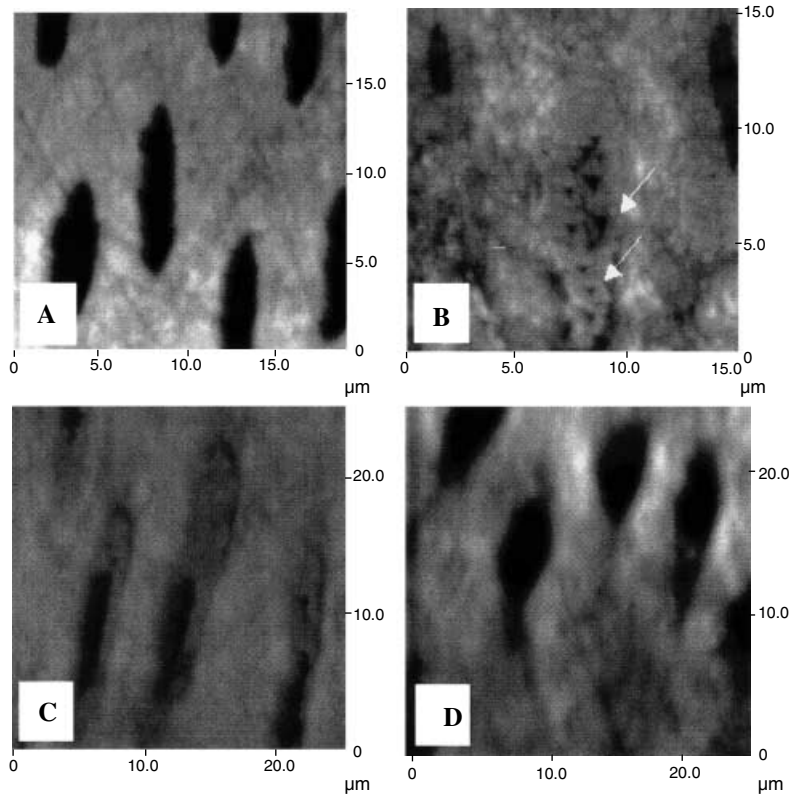


*Fig. 3.* Atomic force microscopy images of different zones typical of arrested carious cases. (A) Image from apparently normal zone, which shows relatively smooth intertubular dentin. The peritubular dentin (PD) was present. (B) Image from the transparent zone. The dentin tubules were occluded with intratubular mineral (ITM). The arrows show the indentations within the peritubular dentin. (C) Image from the light pink zone, in which dentin tubules were partly filled with ITM. (D) Image from the pink zone, which contained neither PD nor ITM.

*Planar data set* – The dependence of hardness and reduced elastic modulus of intertubular dentin on caries status and zone were modeled as above, with tooth included as a random effect to correct variance estimates for measurements at multiple indentation sites per tooth. Similar analyses were performed for measurements made in the PD and ITM.

## Results

The elastic modulus and hardness were highly correlated (linear data,  $\text{corr} = 0.95$ ; planar data,  $\text{corr} = 0.87$ ).

As indicated above, all carious lesions in the eight teeth extended into the dentin, but were extended no more than about 75% of the dentinal depth. Fig. 1A shows the low-magnification digital image of an arrested carious dentin lesion stained by Caries Detector. The lesion was divided into four zones based on the staining: pink, light pink, transparent, and apparently normal zone. Fig. 1B shows another arrested carious stained sample; externally the carious lesion appeared to be dark brown, and the prepared section barely stained with Caries Detector. Fig. 2A shows the low-magnification digital image of a tooth with moderately active carious unstained dentin. The unstained lesion was slightly discolored and seemed to be softer than arrested carious

lesions; some tissue was lost due to the caries. Fig. 2B shows moderately active carious lesion after staining. The lesion stained more intensely than arrested carious cases.

Figs. 3A and 4A show the AFM images from the apparently normal zones below the transparent zone of arrested and moderately active carious lesions. Lesions in both groups had relatively smooth intertubular dentin, and peritubular dentin was present. The arrow in Fig. 4A shows a typical indentation within the peritubular dentin of a moderately active case. Figs. 3B and 4B show AFM images from the transparent region of arrested and moderately active carious lesions, respectively. The dentinal tubules were occluded with intratubular mineral in all cases in both groups. The arrows in Fig. 3B show the indentations in PD and ITM for an arrested carious case. Figs. 3C and 4C show the AFM images from the light pink zones of the two groups, in which dentinal tubules were partly filled with intratubular mineral, but peritubular dentin appeared to be partly dissolved. The microstructure of the pink zone contained neither PD nor ITM for both lesion groups, as shown in Figs. 3D and 4D for arrested and moderately active carious cases, respectively. In addition the intertubular dentin appeared to have a different texture, presumably owing to low mineral content compared with that in the apparently normal zone as shown in

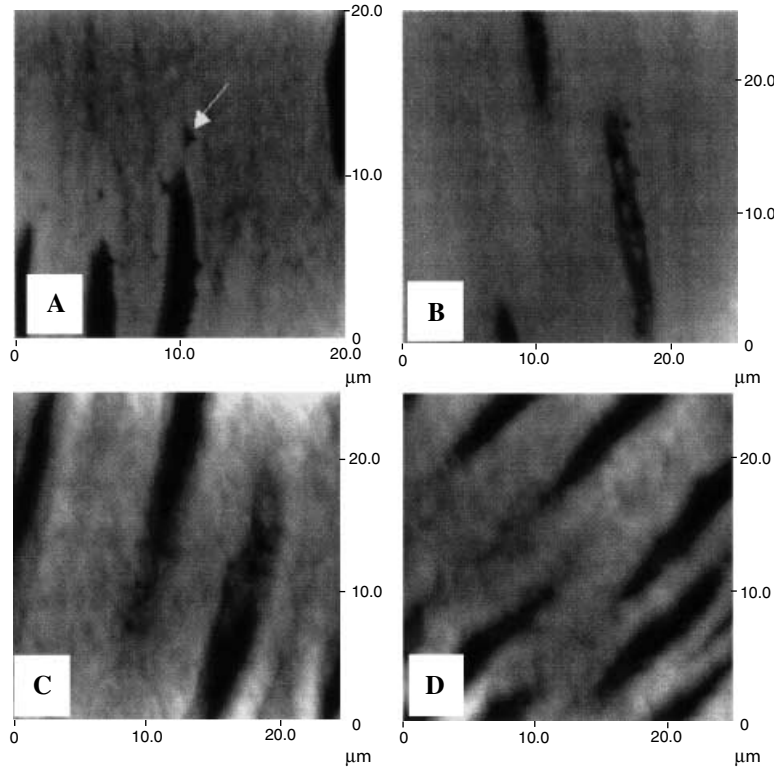


Fig. 4. Atomic force microscopy images of different zones typical of moderately active carious cases. Characteristics of each zone were similar to those seen in the arrested cases in Fig. 3. (A) Image from apparently normal zone, which shows relatively smooth intertubular dentin. The arrow indicates a typical indentation within the peritubular dentin (PD) of a moderately active case. (B) Image from the transparent zone, in which the dentin tubules were occluded with intratubular mineral (ITM). (C) Image from the light pink zone, in which dentin tubules were partly filled by ITM; the peritubular dentin appeared to be partly dissolved. (D) Image from the pink zone. The microstructure of the pink zone contained neither PD nor ITM for both lesion groups. The intertubular dentin appeared to have a different texture, owing to low mineral content compared with that in the apparently normal zone as shown in (A).

Figs. 3A and 4A. This was true of both lesion types and the microscopic appearance of each zone was very similar in the arrested and moderately active carious cases.

Fig. 5 shows that the pink zone occupied over half of the dentin depth in teeth with moderately active carious lesions (57%), and the underlying light pink zone (9%), transparent zone (10%), and apparently normal zone (< 20%) were relatively narrow. In teeth with arrested lesions, the pink zone was shallower (33%) but the light pink zone (19%) and transparent zone (16%) occupied greater fractions of the dentin depth than in teeth with moderately active lesions.

**Linear data set**

Fig. 6A shows both hardness and reduced elastic modulus in the intertubular dentin from the external pink zone through the other zones to the apparently normal zone for the arrested carious lesion shown in Fig. 1A. Fig. 6B shows both hardness and reduced elastic modulus across the pink zone towards the apparently normal zone for the intertubular dentin from the moderately active carious case seen in Fig. 2A. Fig. 7A shows the average hardness and Fig. 7B shows the average modulus from the intertubular dentin for the four lesions of

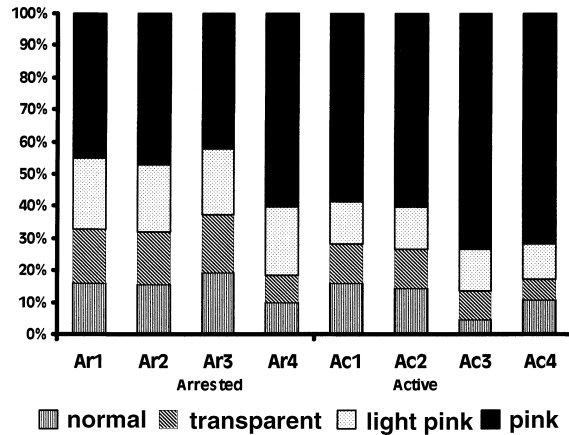


Fig. 5. Percentage of dentin occupied by each zone for the eight carious lesions categorized into arrested or moderately active types. Ar, arrested; Ac, moderately active.

each caries type. Both properties increased from the pink zone towards the apparently normal zone. In the arrested caries specimens, the increases began at the DEJ; by the 50th percentile of the DEJ-to-pulp length, hardness had reached 0.5 GPa and reduced elastic modulus had

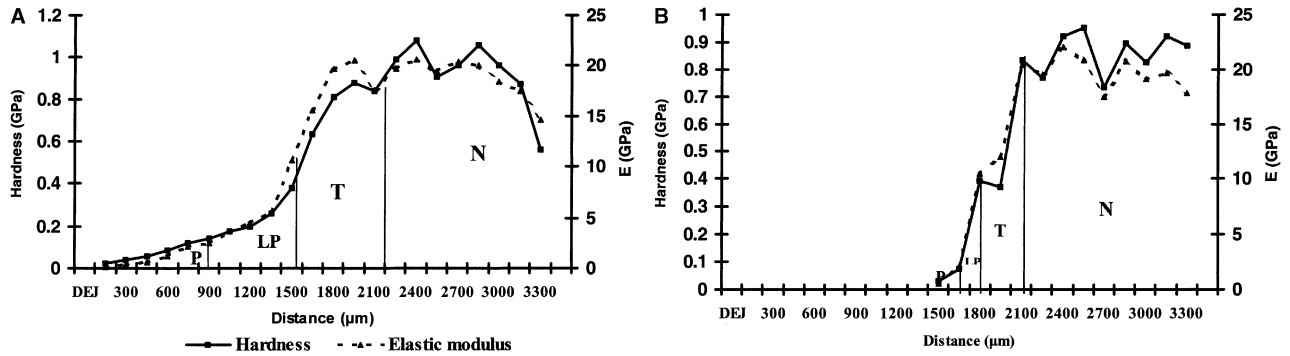


Fig. 6. Hardness and reduced elastic modulus ( $E$ ) in the intertubular dentin for individual carious specimens. Vertical lines divide the lesions into various zones: P, pink; LP, light pink; T, transparent; N, apparently normal. (A) Shows both the hardness and reduced elastic modulus from the external pink zone through the other zones to the apparently normal zone for the arrested carious lesion shown in Fig. 1A. (B) Shows the both hardness and reduced elastic modulus from the external pink zone towards the apparently normal zone for the moderately active carious case seen in Fig. 2A.

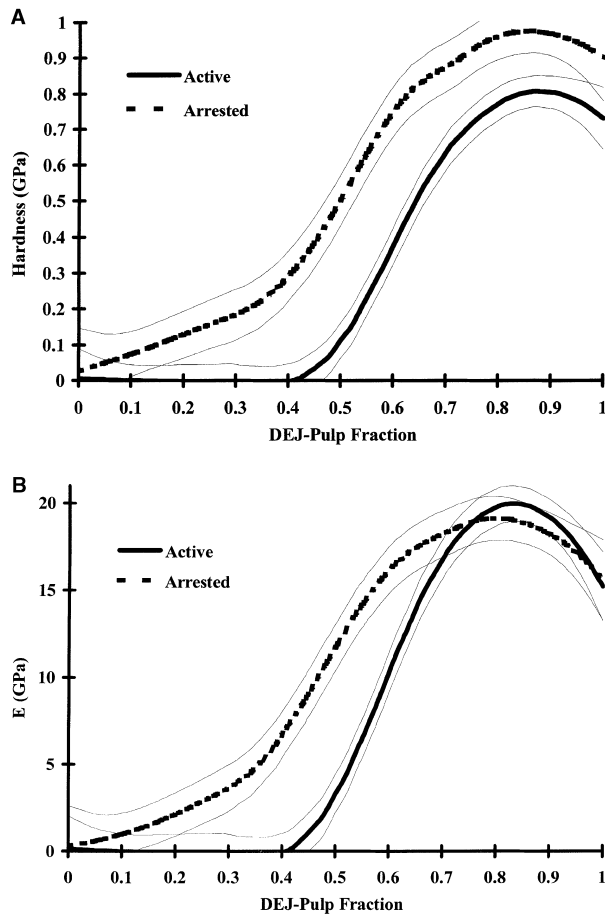


Fig. 7. Average curves with 95% confidence interval (CI) for hardness for the moderately active and arrested caries groups. Data was obtained by using a normalized length scale of 0–100% for the distance from the dentino-enamel junction to pulp using the linear data set from all lesions. (A) Average hardness with 95% CI for the two carious lesion groups. (B) Average reduced elastic modulus with 95% CI for the two carious lesion groups.

reached 12 GPa. In moderately active caries specimens, the increases began nearer the 50th percentile, by which depth hardness had reached 0.1 GPa and reduced elastic modulus had reached 3 GPa. The change from the pink zone towards the apparently normal zone was steeper than that of arrested cases.

Although the mechanical properties of arrested and moderately active caries specimens differed substantially by dentinal depth, the figures suggest that each property was similar across groups within a given zone. For hardness, this was true for the light pink and transparent zones; however, in the apparently normal zone hardness was significantly lower in moderately active compared with the arrested caries specimens ( $P < 0.001$ , linear data set;  $P = 0.012$ , planar data set, Table 1). The hardness values of the transparent zones were significantly lower than the underlying apparently normal zones ( $P < 0.001$ , Table 1).

In contrast, the reduced elastic modulus levels were, on average, higher in active than arrested caries specimens in the light pink zone and transparent zone ( $P < 0.05$ , linear data set, Table 2). However, when the properties were measured at randomly identified locations (planar data set) in the intertubular dentin, reduced elastic modulus levels in active caries specimens in the light pink and transparent zone were not significantly greater, as in the linear data set ( $P > 0.40$ , Table 2). Significant differences between the transparent zones and apparently normal zones for reduced elastic modulus were found in the arrested caries specimens ( $P < 0.001$ , Table 2), but not in the moderately active caries specimens ( $P > 0.05$ , Table 2).

The measurements made in the peritubular dentin for moderately active caries compared with arrested caries showed decreased hardness that was just below statistical significance in the transparent and apparently normal zones (Table 1), and no significant decrease in modulus in the transparent zone or normal zones (Table 2). Intratubular mineral in the transparent zone was softer (Table 1) and had a lower modulus (Table 2) in the moderately active cases compared with the arrested cases.

Table 1  
Nano-hardness of carious dentin: moderately active vs. arrested (GPa)

Zone	Moderately active caries		Arrested caries		Difference Mean ± SD	Two-sided <i>P</i> -value (Wald test)
	<i>n</i>	Mean ± SD	<i>n</i>	Mean ± SD		
Linear data, intertubular dentin						
Pink	51	0.02 ± 0.02	28	0.13 ± 0.02	0.11 ± 0.03	0.004
Light pink	8	0.37 ± 0.04	17	0.30 ± 0.03	-0.07 ± 0.05	0.16
Transparent	9	0.65 ± 0.04	14	0.72 ± 0.03	0.07 ± 0.05	0.14
Apparently normal	25	0.80 ± 0.03	30	0.97 ± 0.02	0.17 ± 0.04	< 0.001
Planar data, intertubular dentin						
Pink	45	0.07 ± 0.04	56	0.10 ± 0.038	0.03 ± 0.06	0.62
Light pink	55	0.24 ± 0.04	48	0.23 ± 0.039	-0.01 ± 0.06	0.85
Transparent	49	0.65 ± 0.04	50	0.71 ± 0.039	0.06 ± 0.06	0.34
Apparently normal	82	0.77 ± 0.04	82	0.94 ± 0.037	0.18 ± 0.05	0.012
Planar data, peritubular dentin						
Pink	0	-	5	0.21 ± 0.16	-	-
Light pink	58	0.32 ± 0.07	48	0.48 ± 0.07	0.16 ± 0.10	0.15
Transparent	62	0.92 ± 0.07	52	1.14 ± 0.07	0.22 ± 0.10	0.060
Apparently normal	85	1.08 ± 0.07	41	1.31 ± 0.08	0.23 ± 0.10	0.058
Planar data, intratubular mineral						
Pink	0	-	2	0.26 ± 0.37	-	-
Light pink	0	-	13	0.65 ± 0.17	-	-
Transparent	66	0.67 ± 0.11	53	1.08 ± 0.12	0.40 ± 0.160	0.045
Apparently normal	0	-	0	-	-	-

Table 2  
Reduced elastic modulus of carious dentin: moderately active vs. arrested (GPa)

Zone	Moderately active caries		Arrested caries		Difference Mean ± SD	Two-sided <i>P</i> -value (Wald test)
	<i>n</i>	Mean ± SD	<i>n</i>	Mean ± SD		
Linear data, intertubular dentin						
Pink	51	0.4 ± 0.5	28	2.0 ± 0.5	1.6 ± 0.7	0.04
Light pink	8	10.5 ± 0.8	17	6.8 ± 0.6	-3.7 ± 1.0	< 0.001
Transparent	9	18.0 ± 0.8	14	16.0 ± 0.6	-1.9 ± 1.0	0.063
Apparently normal	25	18.9 ± 0.6	30	18.7 ± 0.5	-0.2 ± 0.8	0.78
Planar data, intertubular dentin						
Pink	45	2.2 ± 0.8	56	2.7 ± 0.8	0.4 ± 1.2	0.71
Light pink	55	7.9 ± 0.8	48	7.9 ± 0.8	0.0 ± 1.2	0.98
Transparent	49	18.3 ± 0.8	50	19.3 ± 0.8	1.0 ± 1.2	0.44
Apparently normal	82	19.1 ± 0.8	82	21.0 ± 0.8	2.0 ± 1.1	0.12
Planar data, peritubular dentin						
Pink	0	-	5	5.7 ± 2.4	-	-
Light pink	58	9.7 ± 1.3	48	12.0 ± 1.4	2.3 ± 1.9	0.26
Transparent	62	23.5 ± 1.3	52	25.1 ± 1.4	1.6 ± 1.9	0.42
Apparently normal	85	23.6 ± 1.3	41	25.0 ± 1.4	1.5 ± 1.9	0.47
Planar data, intratubular mineral						
Pink	0	-	2	6.2 ± 3.8	-	-
Light pink	0	-	13	14.0 ± 1.5	-	-
Transparent	66	23.0 ± 0.7	53	26.2 ± 0.7	3.2 ± 1.0	0.001
Apparently normal	0	-	0	-	-	-

**Discussion**

The hardness of carious dentin has been studied by a number of researchers using microindentation techniques (6,8,23,24). The relatively large load (50 g) and indenter size of the microindentation technique yield values that represent an average of the composite

microstructures for the dentin structure. Moreover, all of the measurements were performed under dry conditions, and any demineralized matrix, such as found in carious lesions, will shrink until it is supported by the underlying mineralized dentin (6,12,25,26). Therefore, the values for such demineralized dentin may not be representative of the characteristic mechanical properties of the carious

lesion. Because AFM allows high-resolution imaging and site-specific measurements of both hardness and reduced elastic modulus in hydrated samples, MARSHALL *et al.* (7) used this method to determine the hardness and reduced elastic modulus of carious zones, but did not classify the activity status of dentin caries. In this study, we divided the carious lesions into moderately active and arrested caries categories according to their color change, consistency, and staining with Caries Detector. For the moderately active caries, the pink zone occupied more than half the lesion (Fig. 5); the mean values of reduced hardness and elastic modulus were 0.07 GPa and 2.2 GPa, respectively (planar data set). Since much of the pink zone was too soft to make reliable measurements, the true average hardness is probably lower, and therefore the values described above for the pink zone are an upper bound (Figs. 6B and 7); however, since the values could be obtained across the pink zone in arrested caries specimens (Figs. 6A and 7), both hardness (0.1 GPa) and reduced elastic modulus (2.7 GPa) may be representative of the mechanical properties of this zone. Clinical observations have indicated that the arrested lesions appeared to be harder than the moderately active lesions, and our current results confirmed these studies.

Both data sets showed that the intertubular dentin in the apparently normal zones beneath the carious lesion had significantly lower hardness in the moderately active than in the arrested caries ( $P < 0.001$ , Table 1). Therefore, the underlying apparently normal dentin beneath the carious lesion in the moderately active carious cases has probably been demineralized by the carious process, although no significant difference was found between the two types of apparently normal zones for reduced elastic modulus ( $P > 0.05$ , Table 2).

The previous microhardness data indicated that the transparent zone was softer than underlying apparently normal dentin (6), even though most of the tubule lumens were filled with intratubular mineral. By using AFM, MARSHALL *et al.* (7) reported that the transparent intertubular dentin was partly demineralized, but the reduced elastic properties of the microstructure were apparently unchanged. The current study indicated that the transparent dentin existed in both types of caries lesion, and the mean hardness of transparent intertubular dentin was found to be significantly lower than the underlying apparently normal dentin in both moderately active and arrested carious specimens ( $P < 0.001$ , Table 1) because of dissolution of mineral. However, the mean reduced elastic modulus of the transparent zone was not significantly different from its underlying apparently normal zone in the moderately active carious cases ( $P = 0.24$ , linear data;  $P = 0.08$ , planar data; Table 2). KUBOKI *et al.* (27) demonstrated that intermolecular crosslinks of collagen fibrils still remained in this zone, and collagen fibrils were present with distinct crossbanding and interbands (2,3). These results further support the idea that the transparent zone can be remineralized, if its lost mineral and apatite crystals can be reincorporated; thus, it should be preserved in clinical treatment. Interestingly, the modulus was not

significantly different for a given zone, except perhaps for the pink zone, because of probable selection bias, as discussed previously. The similarity in the elastic properties of the regions that could be measured suggests that the processes occurring in each zone are similar in both moderately active and arrested cases. The results in this study differed somewhat with previous work (7), since they found only a slight decrease in hardness and modulus for intertubular dentin compared with normal dentin. Our results were similar for the arrested lesions, and the more active lesions were probably not evaluated in the earlier work.

The light pink transition zone between the pink zone and the transparent zone had significantly lower values for hardness and reduced elastic modulus of the intertubular dentin compared with the transparent zone ( $P < 0.001$ ). Since a turbid zone was reported lying superficial to the transparent zone (28), the light pink zone might correspond to this zone.

The outer pink zone showed the lowest values among the four zones, and it reportedly has been invaded by bacteria (28), lost the interband structure of collagen fibrils (2), and has intermolecular collagen cross-links that are irreversibly broken (27). The pink zone was considered as the outer layer, which traditional treatment concepts suggest should be removed for carious treatment (28). Recently, the traditional treatment for carious lesions has been challenged, and at least some portions of significantly demineralized zones also seemed to be remineralizable (5,29). By using stepwise excavation and calcium hydroxide for treatment of deep carious lesions, slightly discolored soft lesions appear to become arrested and the bacterial counts decrease significantly (30,31).

For the PD, the hardness and reduced elastic modulus in the transparent zone did not show any significant difference compared with the PD in the underlying apparently normal dentin ( $P > 0.05$ ). Since the PD, which might have been partly demineralized in the transparent zone, is narrow and difficult to measure, it is possible that sites selected for measurement were more intact and less demineralized than other areas that were not measured. Thus, these results must be interpreted with some caution. However, the peritubular dentin seems to have minimal influence on the overall mechanical properties of dentin (32); thus, this point may not have an important practical impact. In the light pink zone, both hardness and reduced elastic modulus of PD were reduced significantly ( $P < 0.001$ ). In the pink zone, PD almost disappeared owing to dissolution.

FRANK & VOGEL (33) reported that inorganic crystallite deposits in the tubule lumens consisted of whitlockite, with hydroxyapatite present at later stages. The occlusion of the tubule lumens leads to the formation of the transparent zone. Intratubular mineral was mainly present in the light pink zones of arrested and transparent zones of both moderately active and arrested lesions. For the light pink zones in moderately active caries, because the intratubular mineral only partly filled the tubular lumen, the indentations could not consistently be made reliably. For arrested caries, it is assumed that the process

of remineralization is faster than demineralization, and therefore the values of hardness and reduced elastic modulus for intratubular mineral in the transparent zone for the arrested caries were significantly higher than those for the moderately active caries (hardness:  $P < 0.05$ ; reduced elastic modulus:  $P < 0.001$ . Tables 1 and 2). The intratubular mineral in the light pink zone for arrested caries was found to be softer than that in the deeper transparent zone (hardness  $P < 0.05$ ; reduced elastic modulus  $P < 0.001$ ). This might be because demineralization gradually decreased with depth. The previously reported lower microhardness data for the transparent zone (6) indicated that filling the tubule lumen with mineral does not enhance the mechanical properties (7). In clinical bonding procedures, these intratubular mineral deposits appeared to be more acid resistant (28,34), thus stronger acids or longer etching times may be needed for solubilization to create more resin tags for high bond strengths (35,36). Finally, it should be noted that the carious lesions contained the same zones, regardless of activity status. Different zones exhibited different mechanical properties; the transparent zone existed in both types of caries, and was softer, but had no significant difference in reduced elastic modulus compared with the underlying apparently normal zone for active carious cases. The outer layer in arrested carious lesions was usually harder than that in moderately active carious lesions. The major differences found in this comparison of moderately active and arrested lesions included a steeper increase in mechanical properties and larger areas of the pink zone in the moderately active cases.

*Acknowledgements* – This work was supported by NIH/NID-CR Grant P01 DE09859. The authors gratefully acknowledge Grace Nonomura for her assistance in collecting carious teeth and Vickie Leow for taking the digital images.

## References

- FUSAYAMA T. Two layers of carious dentin; diagnosis and treatment. *Oper Dent* 1979; **4**: 63–70.
- OGUSHI K, FUSAYAMA T. Electron microscopic structure of the two layers of carious dentin. *J Dent Res* 1975; **54**: 1019–1026.
- SHIMIZU C, YAMASHITA Y, ICHIJO T, FUSAYAMA T. Carious change of dentin observed on longspan ultrathin sections. *J Dent Res* 1981; **60**: 1826–1831.
- TEN CATE JM. Remineralization of caries lesions extending into dentin. *J Dent Res* 2001; **80**: 1407–1411.
- MALTZ M, DE OLIVEIRA EF, FONTANELLA V, BIANCHI R. A clinical, microbiologic, and radiographic study of deep caries lesions after incomplete caries removal. *Quintessence Int* 2002; **33**: 151–159.
- OGAWA K, YAMASHITA Y, ICHIJO T, FUSAYAMA T. The ultrastructure and hardness of the transparent layer of human carious dentin. *J Dent Res* 1983; **62**: 7–10.
- MARSHALL GW, HABELITZ S, GALLAGHER R, BALOOCH M, BALOOCH G, MARSHALL SJ. Nanomechanical properties of hydrated carious human dentin. *J Dent Res* 2001; **80**: 1768–1771.
- HOSOYA Y, MARSHALL SJ, WATANABE LG, MARSHALL GW. Microhardness of carious deciduous dentin. *Oper Dent* 2000; **25**: 81–89.
- FUSAYAMA T, TERACHIMA S. Differentiation of two layers of carious dentin by staining. *J Dent Res* 1972; **51**: 866.
- SANO H. Relationship between caries detector staining and structural characteristics of carious dentin. *J Stomatol Soc Jpn* 1987; **54**: 241–270.
- KIDD EA, JOYSTON-BECHAL S, BEIGHTON D. The use of a caries detector dye during cavity preparation: a microbiological assessment. *Br Dent J* 1993; **174**: 245–248.
- MARSHALL GW JR, MARSHALL SJ, KINNEY JH, BALOOCH M. The dentin substrate: structure and properties related to bonding. *J Dent* 1997; **25**: 441–458.
- BALOOCH M, WU-MAGIDI IC, BALAZS A, LUNDKVIST AS, MARSHALL SJ, MARSHALL GW, SIEKHAUS WJ, KINNEY JH. Viscoelastic properties of demineralized human dentin measured in water with atomic force microscope (AFM)-based indentation. *J Biomed Mater Res* 1998; **40**: 539–544.
- CUY JL, MANN AB, LIVI KJ, TEAFORD MF, WEIHS TP. Nanoindentation mapping of the mechanical properties of human molar tooth enamel. *Arch Oral Biol* 2002; **47**: 281–291.
- KINNEY JH, BALOOCH M, MARSHALL SJ, MARSHALL GW JR, WEIHS TP. Atomic force microscope measurements of the hardness and elasticity of peritubular and intertubular human dentin. *J Biomech Eng* 1996; **118**: 133–135.
- KINNEY JH, BALOOCH M, MARSHALL SJ, MARSHALL GW JR, WEIHS TP. Hardness and Young's modulus of human peritubular and intertubular dentine. *Arch Oral Biol* 1996; **41**: 9–13.
- MARSHALL SJ, BALOOCH M, BREUNIG T, KINNEY JH, TOMSIA AP, INAI N, WATANABE LG, WU-MAGIDI IC, MARSHALL GW. Human dentin and the dentin–resin adhesive interface. *Acta Mater* 1998; **46**: 2529–2539.
- HABELITZ S, MARSHALL SJ, MARSHALL GW JR, BALOOCH M. Mechanical properties of human dental enamel on the nanometre scale. *Arch Oral Biol* 2001; **46**: 173–183.
- WHITE JM, GOODIS HE, MARSHALL SJ, MARSHALL GW. Sterilization of teeth by gamma radiation. *J Dent Res* 1994; **73**: 1560–1567.
- HABELITZ S, MARSHALL GW, BALOOCH M, MARSHALL SJ. Nanoindentation and storage of teeth. *J Biomech* 2002; **35**: 995–998.
- DOERNER MF, NIX WD. A method for interpreting the data from depth-sensing indentation instruments. *J Mater Res* 1986; **1**: 601–609.
- OLIVER WC, PHARR GM. An improved technique for determining hardness and elastic modulus using load and displacement sensing indentation experiments. *J Mater Res* 1992; **7**: 1564–1583.
- CRAIG RG, PEYTON FA. The microhardness of enamel and dentin. *J Dent Res* 1958; **37**: 661–668.
- FUSAYAMA T, OKUSE K, HOSODA H. Relationship between hardness, discoloration, and microbial invasion in carious dentin. *J Dent Res* 1966; **45**: 1033–1046.
- KANCA J 3RD. Resin bonding to wet substrate. 1. Bonding to dentin. *Quintessence Int* 1992; **23**: 39–41.
- KANCA J 3RD. Effect of resin primer solvents and surface wetness on resin composite bond strength to dentin. *Am J Dent* 1992; **5**: 213–215.
- KUBOKI Y, OHGUSHI K, FUSAYAMA T. Collagen biochemistry of the two layers of carious dentin. *J Dent Res* 1977; **56**: 1233–1237.
- FUSAYAMA T. *A simple restorative system by minimal reduction and total etching*. Ishiyaku-Euro America, Tokyo, Japan, St Louis, USA 1993.
- MERTZ-FAIRHURST EJ, CURTIS JW JR, EGGLE JW, RUEGGERBERG FA, ADAIR SM. Ultraconservative and cariostatic sealed restorations: results at year 10. *J Am Dent Assoc* 1998; **129**: 55–66.
- BJØRNDAL L, LARSEN T, THYLSTRUP A. A clinical and microbiological study of deep carious lesions during stepwise excavation using long treatment intervals. *Caries Res* 1997; **31**: 411–417.
- BJØRNDAL L, LARSEN T. Changes in the cultivable flora in deep carious lesions following a stepwise excavation procedure. *Caries Res* 2000; **34**: 502–508.

32. KINNEY JH, BALOOCH M, MARSHALL GW, MARSHALL SJ. A micromechanics model of the elastic properties of human dentine. *Arch Oral Biol* 1999; **44**: 813–822.
33. FRANK RM, VOEGEL JC. Ultrastructure of the human odontoblast process and its mineralization during dental caries. *Caries Res* 1980; **14**: 367–380.
34. MARSHALL GW JR, CHANG YJ, GANSKY SA, MARSHALL SJ. Demineralization of caries-affected transparent dentin by citric acid: an atomic force microscopy study. *Dent Mater* 2001; **17**: 45–52.
35. NAKAJIMA M, SANO H, BURROW MF, TAGAMI J, YOSHIYAMA M, EBISU S, CIUCCHI B, RUSSELL CM, PASHLEY DH. Tensile bond strength and SEM evaluation of caries-affected dentin using dentin adhesives. *J Dent Res* 1995; **74**: 1679–1688.
36. NAKAJIMA M, SANO H, URABE I, TAGAMI J, PASHLEY DH. Bond strengths of single-bottle dentin adhesives to caries-affected dentin. *Oper Dent* 2000; **25**: 2–10.